MICROBIAL ECOLOGY

Microb Ecol (1999) 37:173–184
DOI: 10.1007/s002489900141

A Microsensor Study of the Interaction between Purple Sulfur and Green Sulfur Bacteria in Experimental Benthic Gradients

O. Pringault,[1] R. de Wit,[1] M. Kühl[2]

[1] Laboratoire d'Océanographie Biologique, Université Bordeaux I, C.N.R.S.-U.M.R. 5805, 2, rue du Prof. Jolyet F-33120 Arcachon, France
[2] Max Planck Institut für Marine Mikrobiologie Microsensor Research Group, Celsiusstrasse 1, D-28359 Bremen, Germany

Received: 15 June 1998; Accepted: 18 January 1999

Abstract

The interaction between the purple sulfur bacterium *Thiocapsa roseopersicina* and the green sulfur bacterium *Prosthecochloris aestuarii* was studied in a gradient chamber under a 16-hours light-8-hours dark regime. The effects of interaction were inferred by comparing the final outcome of a mixed culture experiment with those of the respective axenic cultures using the same inoculation densities and experimental conditions. Densities of bacteria were deduced from radiance microprofiles, and the chemical microenvironment was investigated with O_2, H_2S, and pH microelectrodes. *P. aestuarii* always formed a biofilm below the maximal oxygen penetration depth and its metabolism was strictly phototrophic. In contrast, *T. roseopersicina* formed a bilayer in both the mixed and the axenic culture. The top layer formed by the latter organism was exposed to oxygen, and chemotrophic sulfide oxidation took place during the dark periods, while the bottom layer grew phototrophically during the light periods only. In the mixed culture, the relative density of *P. aestuarii* was lower than in the axenic culture, which reflects the effects of the competition for sulfide. However, the relative density of *T. roseopersicina* was actually higher in the mixed culture than in the corresponding axenic culture, indicating a higher growth yield on sulfide in the mixed culture experiment. Several hypotheses are proposed to explain the effects of the interaction.

Introduction

Phototrophic sulfur bacteria are commonly found in stratified systems within vertical gradients of light and chemical compounds, particularly of sulfide and oxygen. Their proliferation can be very intense in anoxic layers of pelagic or benthic environments if sufficient light is available [49]. Dense blooms of phototrophic sulfur bacteria have been described in the photic zones of stratified lakes [26]. In benthic systems, these microorganisms can grow in the upper millimeters of shallow aquatic sediments. Especially in microbial mats, high population densities are often observed [13, 43, 50].

Correspondence to: O. Pringault, Max Planck Institut für Marine Mikrobiologie, Microsensor Research Group, Celsiusstrasse 1, D-28359 Bremen, Germany; Fax: +49 421 2028 580; E-mail: opringau@mpi-bremen.de

Phenotypically, phototrophic sulfur bacteria are divided in two groups, purple sulfur bacteria (PSB) and green sulfur bacteria (GSB), according to their pigment composition and the location of light-harvesting antennae [14]. Purple sulfur bacteria have bacteriochlorophyll *a* (Bchl *a*), Bchl *b,* and various carotenoids (okenone, spirilloxanthin) incorporated into a complex photosynthetic membrane system continuous with the cell membrane [33]. Green sulfur bacteria mainly contain Bchl *c, d,* or *e* and carotenoids such as chlorobactene and isorenieratene. The light-havesting pigments are carried by special structures called chlorosomes, which represent large and powerful antenna systems and are attached to the inner side of the cytoplasmic membrane [14, 41]. Green sulfur bacteria also contain small amounts of Bchl *a* in the chlorosome [1] and in the photosynthetic reaction centers, which are located in the cytoplasmic membrane at the attachment sites of the chlorosomes.

Purple and green sulfur bacteria exhibit different physiological characteristics. Green sulfur bacteria do not tolerate oxygen [49], whereas most PSB are able to grow chemotrophically with oxygen as electron acceptor [5, 16, 31]. Green sulfur bacteria need less light for their growth and exhibit major light absorption in spectral regions where PSB do not absorb [47]. The mode of CO_2 fixation is also different [42, 44], and the GSB have a higher affinity for sulfide than do the PSB [45]. However, in spite of these physiological differences, GSB and PSB have to be considered competitors for sulfide, which is the main electron donor for both groups of microorganisms.

Studies on the interaction between GSB and PSB have mainly focused on pelagic examples, because liquid cultures provide an appropriate experimental tool for these environments [11, 18, 32]. These studies highlighted the roles of light distribution, oxygen, sulfur compounds, and organic matter in the competition between and the coexistence of PSB and GSB in pelagic systems [47, 51]. In benthic environments, GSB and PSB are living in steep gradients of oxygen, sulfide, and light on a scale of millimeters or less within the sediment [48]. Only a few studies have been performed to determine the roles of physicochemical gradients in the competition between these phototrophic microorganisms, because of the difficulty to experimentally recreate their natural benthic habitats [47, 49].

The objectives of the present research were to study resource use of and the interactions between GSB and PSB in a spatially ordered benthic environment and how the steep solutes and light gradients affect the stratification of their populations. Therefore, a Benthic Gradient Chamber (BGC), recently developed by Pringault et al. [36], was used to culture GSB and PSB. The BGC allows the culturing of phototrophic microorganisms in benthic light, oxygen, sulfide, and pH gradients similar to those observed in their natural habitats [36, 37]. Axenic biofilms of the purple sulfur bacterium *Thiocapsa roseopersicina* and the green sulfur bacterium *Prosthecochloris aestuarii* were compared with a mixed culture of both species cultured under identical conditions. At the end of the incubation time, the depth distribution of bacteria and their light environment were deduced from field radiance and scalar irradiance microprofiles, respectively. The metabolism of the bacteria was analyzed from oxygen, sulfide, and pH profiles measured with microelectrodes.

Materials and Methods

Bacterial Strains

Two strains of nonmotile phototrophic sulfur bacteria from the culture collection of the Laboratory of Biological Oceanography (University Bordeaux I, Arcachon, France) were cultured in the BGC: the purple sulfur bacterium *Thiocapsa roseopersicina* strain EP 2204 and the green sulfur bacterium *Prosthecochloris aestuarii* strain CE 2401. *T. roseopersicina* strain EP 2204 is able to grow photoautotrophically with sulfide, elemental sulfur, thiosulfate, and sulfite as electron donor [12]. This strain can also grow chemolithotrophically with oxygen as electron acceptor [12]. In the case of *P. aestuarii* strain CE 2401, photolithotrophy is possible with sulfide and elemental sulfur, but does not occur with thiosulfate and is inhibited by sulfite [12]. As a strict anaerobe, the green sulfur bacterium lacks the potential of chemotrophic metabolism with oxygen as electron acceptor. During the assemblage of the BGC, the top centimeter of the sand core was inoculated with a small volume (10 ml) from a batch culture in logarithmic growth phase as described in Pringault et al. [36]. For the mixed culture, both strains were inoculated simultaneously under the same conditions applied for the axenic cultures.

Culture Conditions

Axenic cultures and interaction experiments were performed with both bacteria in parallel Benthic Gradient Chamber cultures using the same incubation conditions. The design of the BGC has been described in detail by Pringault et al. [36]; its use in this study is summarized below. The culturing device is composed of a 45-mm-long sand core (internal diameter 40 mm) sandwiched in between an upper oxic and a lower anoxic chamber. The sand (Merck, Germany) had a grain size of 125–250 μm. Transport of solutes through the sand core was exclusively due to molecular diffusion [36]. Oxygen, sulfide, pH, and light gradients were imposed on the system.

The medium in the upper and lower chamber was composed of

reconstituted seawater (Meer Salz, Germany) at a salinity of 35‰, NH_4Cl (5 mM), KH_2PO_4 (0.5 mM), SL12B without EDTA (1ml L^{-1}) [33], and the vitamin solution V7 (1ml L^{-1}) [33].

In the upper oxic medium, oxygen saturation was achieved by providing sterile air via an airlift. Salinity and temperature were maintained constant at 35‰ and 20°C, respectively, during the incubation time. The calculated oxygen concentration in the overlying water at experimental salinity and temperature was 230 μM according to empirical solubility equations [10]. The anoxic lower medium was prepared under a headspace of nitrogen. Na_2S was added to the medium to a final concentration of 40 mM. Owing to a long diffusion path (45 mm) and a large volume of the lower compartment (2400 ml), the sulfide losses after 5 weeks of incubation were minimal (6% of the initial concentration). The lower chamber thus acted as a virtually constant source for sulfide during the experiments.

The pH of the upper compartment was around 8.2–8.3, because of the equilibration established between the air and the upper medium amended with 4 mM of $NaHCO_3$. In the lower chamber, a solution of bicarbonate ($NaHCO_3$) was added to a final concentration of 80 mM. The molar ratio of carbonate to sulfide was 2:1 to allow for a complete oxidation of sulfide to sulfate by photolithotrophy, i.e., $2\ HCO_3^- + 1\ H_2S \rightarrow 2\ [CH_2O] + SO_4^{2-}$ [36]. The pH of the lower medium was around 7.4–7.6.

The BGC was illuminated from above by a collimated light beam of an incandescent lamp (100 W, Super Philux R80, Philips) using a regime of 16 h light and 8 h dark. The downwelling scalar irradiance at the sand surface was equal to 800 and 2200 μmol photons $m^{-2}\ s^{-1}$ for visible light (430–700 nm) and near infrared light (NIR: 700–1000 nm), respectively.

Fiber-Optic Microprobes

Light measurements were performed with fiber-optic microprobes connected to an optical spectral mutlichannel analyzer (O-SMA) [19]. The raw spectra were smoothed mathematically to suppress high-frequency noise by using a "Blackman window" low-pass filtering algorithm with a cutoff frequency of 0.05 (Asystant$^+$ software) [19]. The fiber-optic microprobes have been described previously [19, 21, 25, 37]; their uses in this study are summarized below.

Scalar irradiance microprobe. Depth profiles of scalar irradiance were performed by insertion of the sensor through the sand from the surface at a zenith angle of 150° relative to the incident light. Scalar irradiance measurements were normalized to values measured at the sand surface.

The available quantity of light in the BGC at the initial time of incubation was calculated from scalar irradiance measurements performed in sterile sand using identical light conditions as for the culturing of the bacteria. Scalar irradiance was related to the incident light by measuring the downwelling irradiance above a light trap (black well) as described by Lassen et al. [25].

Field radiance microprobe. Depth profiles of backscattered radiance were measured at 150° zenith angle relative to the incident light by penetrating the sand from the surface in vertical steps of 100 μm. Backscattered radiance measurements were normalized to the values measured at the sand surface.

Light Calculations

Because of the concavity of the BGC walls, it was not possible to determine precisely when the probe reached the sand surface during measurement of a light profile. The sand surface was therefore aligned with the maximum scalar irradiance and backscattered radiance values, as observed for light measurements performed in sediments [21, 22, 25].

Profiles of attenuation coefficient for backscattered field radiance were calculated as the rate of change of log-transformed radiance values with depth [17]:

$$K_L = -\frac{\delta(\ln L)}{\delta z} \quad (1)$$

where L represents the field radiance and z the depth. Polynomial functions (seventh- or eighth-order) were fitted to the log transformed (Napierian logarithm) radiance data. The first derivative of these functions with respect to depth corresponds to the vertical distribution of the radiance attenuation coefficient. The attenuation radiance profiles were calculated for wavelengths corresponding to *in vivo* absorption maxima of major photopigments of bacteria cultured in the BGC. The vertical stratification of bacteria was thus deduced from the radiance attenuation profiles according to their specific photopigments [23, 37].

Microsensors

Oxygen, pH, and sulfide profiles were measured with microelectrodes. The calibration procedure for the different types of electrodes was the same as described previously [37]. Details about the characteristics of the microelectrodes are given below.

Oxygen microelectrode. Concentration profiles of oxygen were measured by a Clark-type oxygen microelectrode with a guard cathode [39]. The electrodes had a tip diameter of 10–20 μm and were connected to a picoammeter and a strip chart recorder. The stirring sensitivity was <1% and the 90% response time was <1 s.

pH microelectrode. Profiles of pH were measured by a pH glass microelectrode [40] connected to a high-impedance electrometer with a calomel electrode (Radiometer) as a reference. The pH microelectrodes had a log-linear response to $[H^+]$ and the calibration curves exhibited a slope of 53 to 58 mV/pH unit and a 90% response time of <10–20 s.

Hydrogen sulfide microsensor. Concentration profiles of dissolved hydrogen sulfide profiles were measured by a new amperometric H_2S microelectrode [15, 24]. The electrodes had a tip diameter of 10–20 μm, a 90% response time <1–2 s, and a stirring sensitivity of <1–2%. The measuring circuit was composed of a picoammeter using a polarization voltage of +85 mV.

Measurements were made with a H_2S and a pH microelectrode

mounted on the same manually operated micromanipulator (Märtzhaüser, Germany). The tips of the pH and sulfide electrodes were positioned <2 mm apart in the same horizontal plane. Oxygen profiles were measured with a microelectrode mounted in a separate manually operated micromanipulator. All measurements were made within the same 1 cm^2 of the sand area with a vertical step size of 100 μm.

Calculations of Solute Fluxes and Metabolic Processes

The depth distribution of metabolic processes and molecular diffusion were inferred from steady-state oxygen and sulfide profiles. In the BGC sand core, the one-dimensional diffusion of a solute compound $J(x)$ is governed by Fick's first law of diffusion applied to the sediment [2]:

$$J(x) = -\phi D_s \frac{\delta C(x)}{\delta x} \quad (2)$$

where ϕ is the porosity, D_s is the sedimentary diffusion coefficient, and C is the solute concentration at position x. The ϕD_s values used were calculated as described by Pringault et al. [36] and equal to 0.694×10^{-5} cm^2 s^{-1} and 0.528×10^{-5} cm^2 s^{-1} for oxygen and sulfide, respectively. Sulfide flux was inferred from the linear part of the sulfide profile. For the oxygen, the flux was calculated from the gradient across the sand–water interface as described by Rasmussen and Jørgensen [38].

The location of the reaction zone was indicated by the curved part of the profile. Metabolic process rates were assumed to be zero-order and, therefore, calculated by quadratic regression [20, 28].

Microsensor measurements were performed after an incubation time of 5 weeks. The closed system was at this time opened to allow the insertion of optical and chemical microsensors. The possible contamination of the system due to the opening was checked by counting cells using microscopic observations. The contaminant cells represented less than 5% of the total cells per field of counting.

Results

Scalar irradiance distribution

The granulometry and the nature of the sand play a fundamental role in the vertical distribution of the scalar irradiance due to the scattering and absorption properties of quartz particles [21, 22]. To determine the quantity of light available for growth in the sand at the beginning of the bacterial culture, scalar irradiance measurements were performed in sterile sand (Fig. 1). At the sand surface, scalar irradiance for 800 nm increased up to 280% of the downwelling scalar irradiance because of high scattering (Fig. 1A). The high values observed in the water phase could in part be due to a focus effect of the glass walls of the BGC (Fig. 1A). Below the sand surface, scalar irradiance was attenuated exponentially with depth, to reach 3.5% of the downwelling scalar irradiance at 5 mm. This attenuation was wavelength dependent (Fig. 1B). The highest scalar irradiance attenuations (K_0) were observed for 450–550 nm with a maximal value of 1.55 mm^{-1} at 490 nm. From 500 nm, K_0 decreased, to reach 0.9 mm^{-1} at 900 nm.

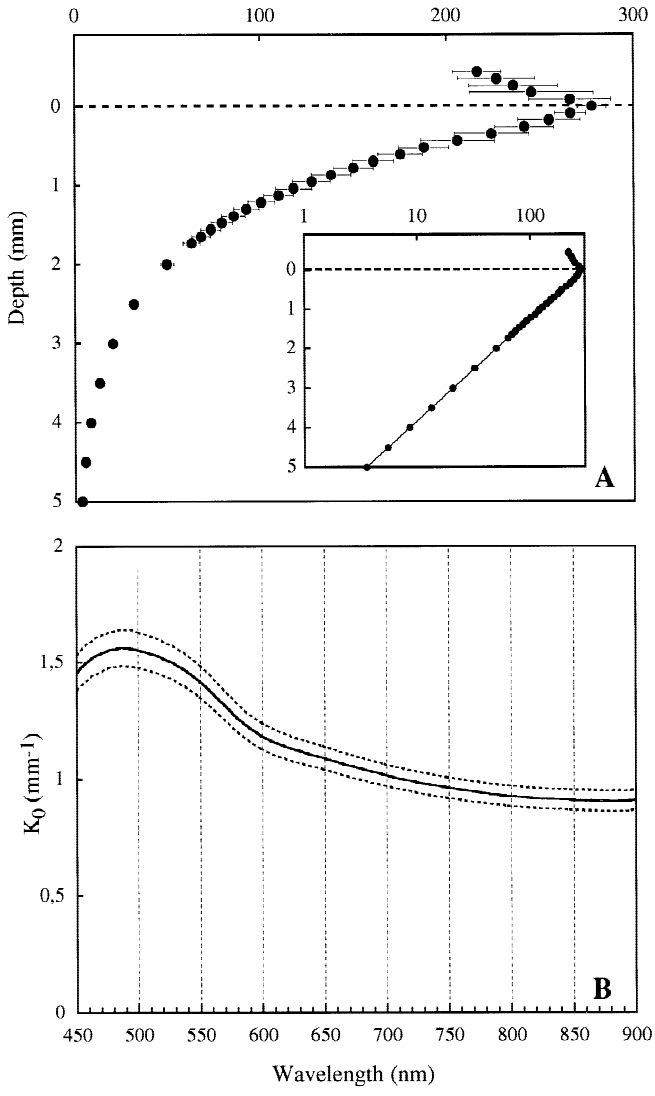

Fig. 1. Scalar irradiance (% of downwelling irradiance) in clean, unpopulated sandy sediment in the BGC illuminated from above by collimated incandescent light (see Methods). (A) Depth profile of 800 nm. Light intensities are expressed as percent of incident irradiance light at the sediment surface. Error bars indicate the standard deviation and data points represent the arithmetic mean of 5 measurements. *Inset* shows log-transformed data. (B) Spectral vertical attenuation coefficient of scalar irradiance, K_0. The spectrum represents the mean of 5 measurements (continuous lines) ± SD (dotted lines).

After 5 weeks of incubation, axenic biofilms of *Thiocapsa*

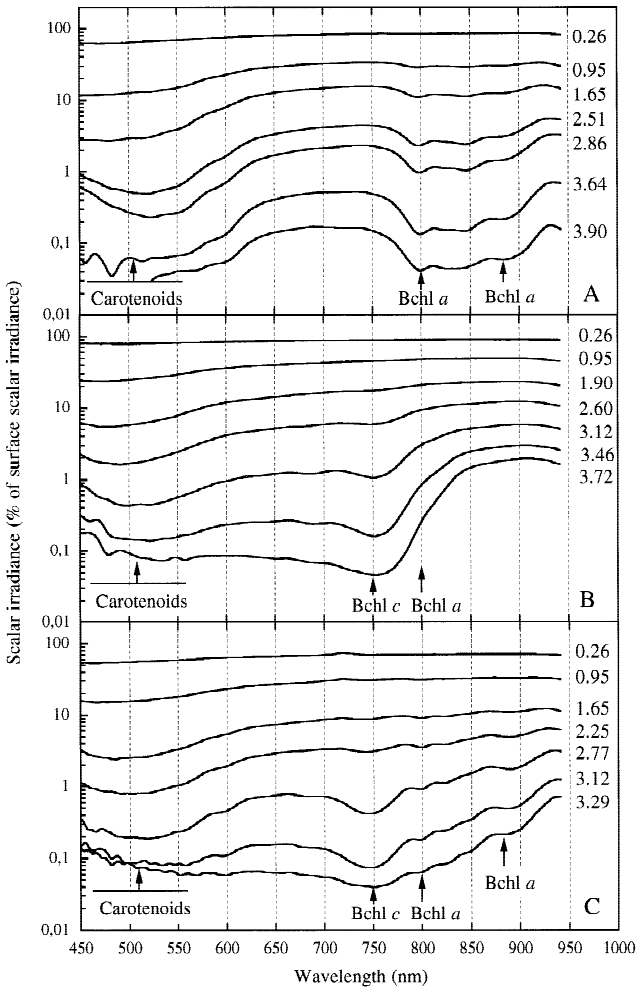

Fig. 2. Scalar irradiance spectra from selected depth (in mm) below the surface (indicated by numbers on graph). (A) Biofilm of *Thiocapsa roseopersicina* strain EP 2204. (B) Biofilm of *Prosthecochloris aestuarii* strain CE 2401. (C) Mixed culture of both bacteria. All cultures were obtained in the BGC (see text for details).

roseopersicina strain EP 2204, *Prosthecochloris aestuarii* strain CE 2401, and a biofilm composed of both were obtained in the BGC within light, oxygen, sulfide, and pH gradients.

The scalar irradiance depth distribution was different according to the cultures (Fig. 2). The purple sulfur and the green sulfur bacteria used different specific wavelengths ranges of the light spectrum for their growth. Between 450 and 550 nm, the scalar irradiance was strongly attenuated in all cultures because of their carotenoids, spirilloxanthin and chlorobactene for *T. roseopersicina* and *P. aestuarii,* respectively [4]. The wavelengths 550–760 nm were preferentially used by the green sulfur bacterium, with a significant peak at 750 nm corresponding to the *in vivo* Bchl *c* maximum (Fig. 2B). The 760–950 nm range was particularly used by *T. roseopersicina,* with maximum attenuations for 800 and 880 nm corresponding to *in vivo* Bchl *a* absorption maxima (Fig. 2A). Hence, the purple and the green sulfur bacteria showed an almost complementary absorption of the light spectrum, which was confirmed by the light measurements in the mixed culture showing strong attenuation over the whole spectrum (Fig. 2C). Scalar irradiance measurements were not really appropriate for tracing the biofilm location because of the size and the optical properties of the scalar irradiance probe. The depth distribution of bacteria was therefore deduced from backscattered radiance profiles.

Biofilm Location

Depth profiles of backscattered radiance for wavelengths corresponding to the major photopigments are shown in Fig. 3. Attenuation profiles were calculated from these radiance measurements as proxies of the depth distribution of the phototrophic bacteria [23, 29, 37].

The radiance attenuation for 800 and 880 nm (Bchl *a*) in the *T. roseopersicina* biofilm showed two small peaks (Fig. 3B). One was located at 1.2 mm with a maximum of 2.2 mm^{-1} and the second at 3.5 mm depth with a maximum value of 4.2 mm^{-1} for 800 nm. Between these two peaks, the radiance attenuation was almost equal to the values for sterile sand. Hence, two populations of *T. roseopersicina* can be distinguished from the attenuation profiles of these two wavelengths. The presence of sulfur globules in the cells could modify the light distribution; hence, the gap between the two population of *T. roseopersicina* might be due to an accumulation of sulfur globules within this sand layer (N. Pfennig, personal communication). Unfortunately, the difficulty of correctly sampling the sand did not allow us to determine the distribution of sulfur compounds via chemical analyses.

In the *P. aestuarii* biofilm, until 2.2 mm below the surface, the radiance attenuation was almost constant with depth for 750 and 800 nm (Figs. 3C and 3D). Below this depth, two peaks were clearly characterized, according to the different bacteriochlorophylls. The spectral signal from Bchl *c* showed maximum values at 3.0 mm, where the attenuation coefficient reached 9.8 mm^{-1} for 750 nm. For 800 nm, the attenuation peaked at 3.2 mm (Fig. 3D). The attenuation profiles for 750 nm and 800 nm provide a good visualization of the location of the *P. aestuarii* biofilm. The gap between the attenuation maxima corresponding to the Bchl *c* and the Bchl *a* indicates that, in the biofilm, the ratio Bchl *c*/Bchl *a* decreased with depth.

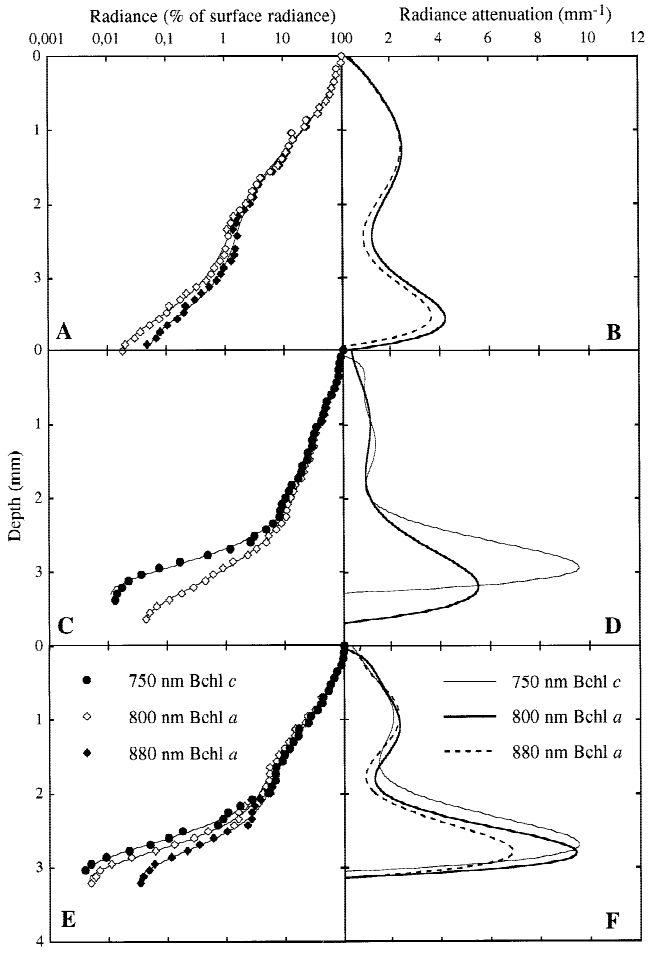

Fig. 3. Radiance measurements in the axenic biofilms of *Thiocapsa roseopersicina* strain EP 2204 (A,B) and *Prosthecochloris aestuarii* strain CE 2401 (C,D), and in mixed culture (E,F). (Left panels) Depth profiles of radiance at absorption wavelengths of major photopigments. Solid lines represent seventh-order polynomials fitted to the data. (Right panels) Depth profiles of attenuation coefficients calculated from the first derivative on log-transformed data.

For the mixed culture, in the first 2 mm spectral signals from both bacteriochlorophylls indicated a dominance of *T. roseopersicina* (Fig. 3F). Below this depth, the backscattered radiance was strongly attenuated (Fig. 3E). The attenuation peaks for the three specific wavelengths were located in the same area, indicating the coexistence of both bacteria. Similar attenuation maxima, 9.3 mm^{-1}, were calculated for 800 and 750 nm. For 880 nm the radiance attenuation maximum was 6.9 mm^{-1}.

Chemical Profiles and Metabolic Activities

Depth profiles of oxygen, sulfide, and pH in the different cultures were measured at the end of the dark and light period (Fig. 4). The metabolic activities, sulfide oxidation and oxygen consumption, and the fluxes for oxygen and sulfide were calculated from these steady-state profiles (Table 1). In the dark, it was possible to detect the thickness of the reaction zone and to calculate the zero-order sulfide oxidation rate from the profile curvature [28]. In contrast, in the light period, the low sensitivity of the H_2S microelectrode at the prevailing pH (8.8–9.0), did not allow a precise location of the reaction zone because of the low amount of dissolved H_2S (less than 1% at pH 8.8). Hence, the sulfide oxidation was deduced from the sulfide fluxes.

In the *T. roseopersicina* biofilm, oxygen and sulfide coexisted at the end of the dark period in a layer 300 μm thick

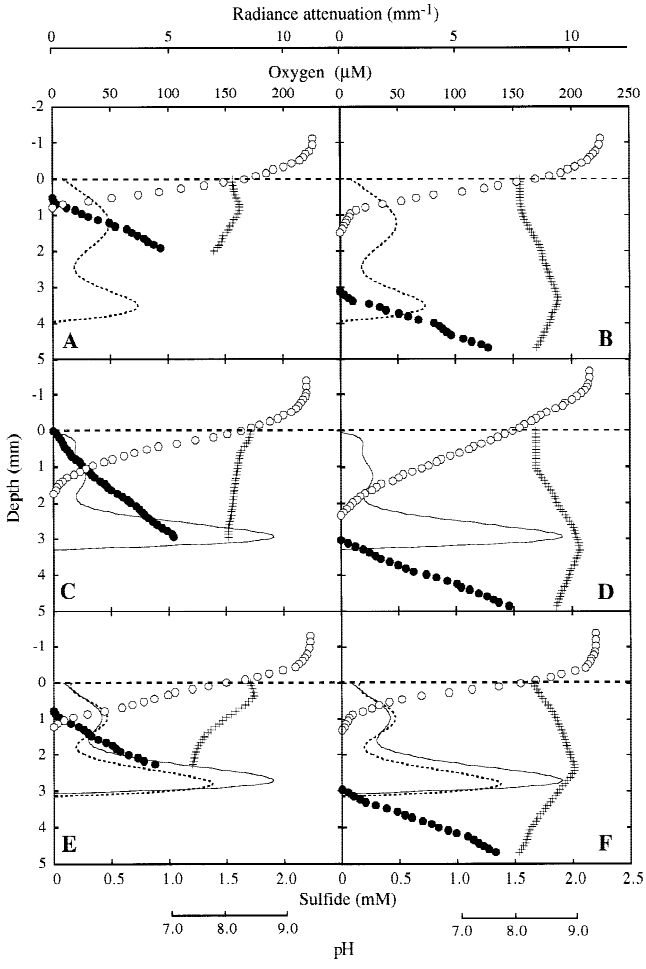

Fig. 4. Oxygen (○), sulfide (●), and pH (+) profiles measured at the end of dark period (left panels) and light period (right panels) both in the axenic biofilms of *Thiocapsa roseopersicina* strain EP 2204 (A,B) and *Prosthecochloris aestuarii* strain CE 2401 (C,D), as well as in mixed culture (E,F). The radiance attenuation for 880 nm (dotted lines) and 750 nm (solid lines) are also depicted to aid in visualizing the bacterial distribution.

Table 1. Oxygen and sulfide fluxes and zero-order reaction rates of O_2 uptake and H_2S oxidation in the axenic biofilms of *Thiocapsa roseopersicina* strain EP 2204, *Prosthecochloris aestuarii* strain CE 2401, and in mixed culture (Com.: compound; n.d.: not determined)

Profile name	Com.	Reaction zone (mm)	Reaction rate ($\mu mol\ cm^{-3}\ h^{-1}$)	Total rate ($\mu mol\ cm^{-2}\ h^{-1}$)	Flux ($\mu mol\ cm^{-2}\ h^{-1}$)
T.	O_2	0.33–0.80	1.11	0.053	0.054
roseopersicina	H_2S	0.49–0.98	2.82	0.138	0.139
end of dark					
T.	O_2	0.85–1.25	0.98	0.041	0.042
roseopersicina		1.25–1.50	0.06		
end of light	H_2S	n.d.[a]	n.d.[a]	n.d.[a]	0.152
P. aestuarii	O_2	0–1.73	0.28	0.048	0.045
end of dark	H_2S	n.d.[b]	n.d.[b]	n.d.[b]	0.131
P. aestuarii	O_2	0.65–2.25	0.12	0.019	0.019
end of light	H_2S	n.d.[a]	n.d.[a]	n.d.[a]	0.163
Coculture	O_2	0.80–1.20	1.03	0.041	0.045
end of dark	H_2S	0.85–1.22	3.24	0.119	0.120
Coculture	O_2	0.20–1.40	0.45	0.054	0.057
end of light	H_2S	n.d.[a]	n.d.[a]	n.d.[a]	0.150

[a] The low sensitivity of the sulfide microelectrode at the prevailing pH (8.8–9.0) did not allow a precise location of the reaction zone from the curved parts of the profile.
[b] The observed kinetics indicated an abiotic sulfide oxidation that cannot be modeled by a zero-order reaction.

(Fig. 4A). The activities deduced from the profiles, 0.053 and 0.138 $\mu mol\ cm^{-2}\ h^{-1}$ for O_2 and H_2S, respectively, were in equilibrium with the influxes by diffusion, 0.054 and 0.139 $\mu mol\ cm^{-2}\ h^{-1}$ for oxygen and sulfide, respectively (Table 1). The sulfide/oxygen consumption ratio was equal to 2.60. This ratio corresponds to the stoichiometry of a sulfide oxidation to elemental sulfur, S^0, via chemosynthetic processes taking into account that one-third of the electrons are used for CO_2 fixation [6]. At the end of light period, the sulfidic zone was shifted downward to below 3 mm depth because of anoxygenic photosynthesis by *T. roseopersicina* (Fig. 4B). The maximum penetration of oxygen was 1.5 mm. The two populations of *T. roseopersicina* were clearly separated by a layer where oxygen and sulfide were not detectable (Fig. 4B). In the light, the sulfide oxidation rate was higher than in the dark period to reach 0.152 $\mu mol\ cm^{-2}\ h^{-1}$ (Table 1).

In the *P. aestuarii* biofilm, at the end of the dark period, oxygen and sulfide coexisted in a 1.8-mm-thick layer (Fig. 4C). The sulfide profile was not in steady state; the observed kinetics could not be modeled by a zero-order model and probably corresponds to abiotic sulfide oxidation processes, which could not equilibrate the high influxes of sulfide by diffusion generated in the BGC (Table 1). Sulfide therefore reached the sand surface (Fig. 4C). At the end of the light period, anoxygenic photosynthetic activity of the bacteria shifted the sulfidic zone down to depths below 3.0 mm. The sulfide oxidation was 0.163 $\mu mol\ cm^{-2}\ h^{-1}$ (Table 1). The biofilm horizon was below the maximum oxygen penetration (2.2 mm), and the radiance attenuation was located in the layer where sulfide and oxygen were not measurable (Fig. 4D).

For the mixed culture, the shapes of the oxygen–sulfide profiles were almost similar to those observed for the *T. roseopersicina* biofilm (Fig. 4E and 4F). In the dark, the coexistence of oxygen and sulfide occurred in a layer of 400 μm (Fig. 4E). The ratio sulfide/oxygen for the activities (Table 1) also indicated an incomplete sulfide oxidation, with elemental sulfur as storage product. In the light, the sulfidic zone shifted downward to below 3 mm depth, whereas the maximal oxygen penetration was 1.3 mm. The sulfide oxidation was 0.150 $\mu mol\ cm^{-2}\ h^{-1}$ (Table 1). The radiance attenuation peaks of *P. aestuarii* and *T. roseopersicina* were located in the layer where oxygen and sulfide were not detectable. The lower limit of the biofilm was positioned at approximately the same depth where the sulfide reached zero during the light period (Fig. 4F).

Discussion

The use of the Benthic Gradient Chamber allowed us to culture phototrophic sulfur bacteria on artificial sand exposed to physicochemical gradients similar to those observed in their natural habitats. The effects of interaction between *T. roseopersicina* and *P. aestuarii* can be inferred by comparing both axenic cultures with the mixed culture of

these phototrophic bacteria. Hence, the axenic cultures were considered as the reference systems. Similar experimental approaches have been developed to study the competition between two rooted phanerogam species grown in monoculture and mixed conditions [5].

The radiance attenuation profiles for specific wavelengths, i.e., 750 nm and 880 nm, provide proxies of the depth distribution of the phototrophic bacteria (Fig. 3): 750 nm corresponds to the *in vivo* absorption maximum of Bchl *c*, specific pigment of *P. aestuarii*, and 880 nm to Bchl *a*, specific to *T. roseopersicina*. The radiance attenuation can be divided into two distinct components: a biotic component corresponding to the bacteria and an abiotic component due to the optical properties of the sand. Accordingly, the radiance attenuation in the axenic biofilms is described by the following equations:

$$K_{PC} = K_P + K_a \quad (3)$$

$$K_{TC} = K_T + K_a \quad (4)$$

where K_{PC} and K_{TC} represent the attenuation in the axenic culture of *P. aestuarii* and *T. roseopersicina*, respectively, equal to the sum of the biotic (K_P for *P. aestuarii* and K_T for *T. roseopersicina*) and the abiotic (K_a) attenuation. Similarly, in the mixed culture, the radiance attenuation for 750 nm and 880 nm can be described by the following equations:

$$K_{MC}(750\text{nm}) = K_P(750\text{nm})x + K_T(750\text{nm})y + K_a(750\text{nm}) \quad (5)$$

$$K_{MC}(880\text{nm}) = K_P(880\text{nm})x + K_T(880\text{nm})y + K_a(880\text{nm}) \quad (6)$$

where K_{MC} represents the attenuation in the mixed culture, and x and y are weighting factors that measure the relative densities in the mixed culture of *P. aestuarii* and *T. roseopersicina*, respectively, by comparison with the corresponding axenic reference culture. The weighting factors x and y are here expressed in arbitrary units (a.u.), where a.u. of x = 1 and a.u. of y = 1 correspond to the maximum density in the axenic cultures. This estimation of the relative density of each species in the mixed culture allowed us to infer interaction effects on the bacterial growth. The relative density of each bacterium according to depth is calculated by solving these two equations using the maximal attenuations for 750 and 880 nm in the axenic reference cultures (Fig. 5).

In the mixed culture, the distribution of the relative densities of both bacteria defines two distinct layers according to depth. In the upper 2 mm, the dominant bacterium was *T. roseopersicina*, whereas *P. aestuarii* was virtually absent in this area. Between 2 and 3.3 mm, both species coexisted, but *P. aestuarii* decreased as compared to the axenic reference culture; the maximum value for x was 0.6. In contrast, *T. roseopersicina* showed a strong increase of its relative density, with a maximum value for y of 2. This clearly indicates, that the mixed culture was advantageous for the purple bacterium and slightly disadvantageous for the green bacterium. However, a fully quantitative interpretation of the outcome of the interaction experiment based on the proximal weighting factors x and y is problematic, because radiance attenuation cannot be converted directly into terms of bacterial biomass for two main reasons. The specific pigment content (i.e., the pigment-to-protein ratio) depends on the bacterial species: GSB generally synthesize more pigments than PSB [49]. Thus, the particularly high attenuation coefficients for 750 nm both in the axenic *P. aestuarii* and in the mixed culture compared to the 880 nm attenuation coefficient for *T. roseopersicina* rather reflected a high specific Bchl *c* content, and not a higher biomass, of *P. aestuarii* (cf. Fig. 3B,D,F). Moreover, the specific pigment content is a function of the light conditions during bacterial growth, i.e., the bacterium increases pigment synthesis with decreasing light availability [9, 30].

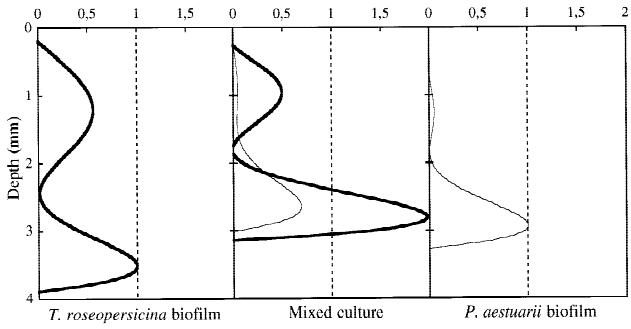

Fig. 5. Relative bacterial density compared to the maximal value in the axenic reference culture (a.u.). Relative density of *Thiocapsa roseopersicina* strain EP 2204 (thick line) and *Prosthecochloris aestuarii* strain CE 2401 (fine line) in the mixed and reference axenic cultures. The relative density, expressed in a.u., is calculated from the maximal attenuation in the axenic reference culture (see text for details).

The observation that *P. aestuarii* exerted a clearly positive effect on *T. roseopersicina* in the experimentally controlled, spatially ordered environment during the incubation period is a new and unanticipated result. Because the negative impact on *P. aestuarii* appears much smaller than the positive effect on *T. roseopersicina*, it shows that in the gradient chamber the mixed culture was more efficient in resource

utilization than the axenic culture. Taking a mixed culture as a highly simplified model of a microbial community, our experimental observations support current ideas that resource utilization is optimized by communities with respect to axenic cultures of their constituent members [3]. The mixed culture exhibited also a more complete spectral depletion of the radiance than the axenic cultures (see Fig. 2), but such a result was not surprising because of the complementary *in vivo* absorption spectra known from liquid cultures. In contrast, the stratification pattern was not fully in agreement with typical textbook predictions, where it is often assumed that green sulfur bacteria stratify below purple sulfur bacteria, because the former have a higher tolerance to sulfide and are capable of growing at lower light intensities. Rather, both bacteria coexisted in the same bottom layer of the mat. Thus, several of the aspects of growth of and interactions between phototrophic bacteria cannot be inferred directly from homogeneous liquid culture experiments, which shows the usefulness of the spatially ordered gradient chamber in microbial ecology. Nevertheless, the stratified mixed culture in the gradient chamber still represents a very complex structure with multiple interactions, which can now be tentatively interpreted in view of previous knowledge of the ecophysiology of *T. roseopersicina* [6, 7, 12, 52], *P. aestuarii* [12], and *Chlorobium* spp., which are physiologically similar to *P. aestuarii* [46, 47, 49]. Hence, the hypothetical interactions between *T. roseopersicina* and *P. aestuarii* in the mixed culture are visualized in the conceptual scheme depicted by Fig. 6. The populations of *P. aestuarii* and *T. roseopersicina* are depicted by boxes, the size and location of which indicate their relative population densities and depth distribution in the sand as described before (cf. Fig. 5).

In the first millimeters, *T. roseopersicina* grew chemosynthetically because of the presence of oxygen, which penetrated down to 1.25 and 1.45 mm in the dark and in the light, respectively (Fig. 6). Although the bacterium was located in the sulfidic zone, sulfide oxidation was incomplete, with intracellular sulfur as the oxidation product, which represents a storage product [7, 8]. After depletion of sulfide, *T. roseopersicina* oxidized its intracellular elemental sulfur to sulfate (Fig. 6B) with oxygen as electron acceptor. The presence of oxygen in this layer inhibited growth of *P. aestuarii.* However, owing to the oxygen consumption via the chemosynthetic processes of *T. roseopersicina,* the green sulfur bacterium was stimulated by the presence of the purple bacterium, which decreased the oxygen penetration depth by comparison with the axenic culture (Fig. 4).

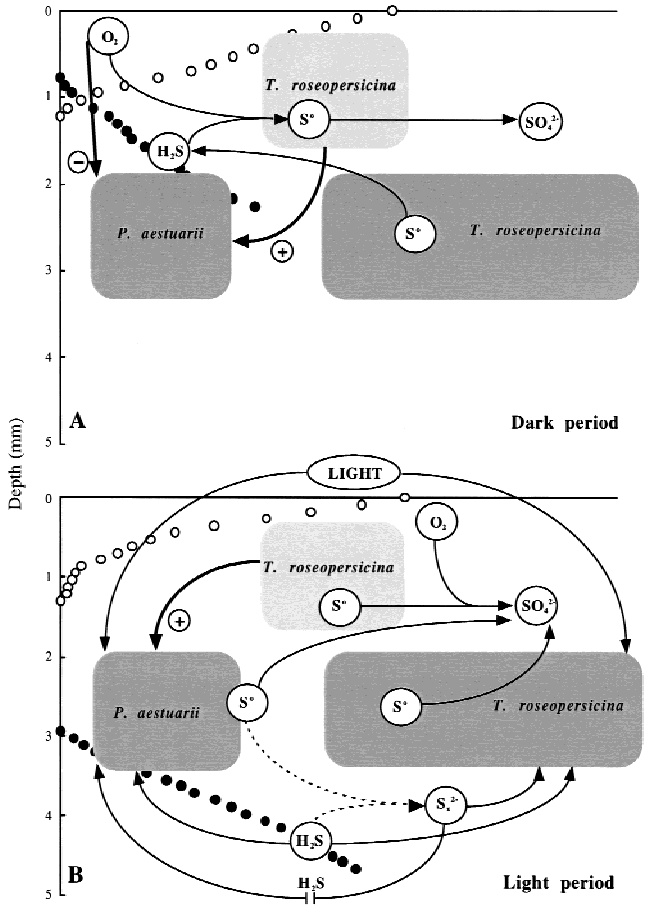

Fig. 6. (A,B) Schematic representation of the interactions involved in the coexistence of *Thiocapsa roseopersicina* strain EP 2204 and *Prosthecochloris aestuarii* strain CE 2401 when cultured in the BGC within experimentally imposed gradients of radiance, oxygen and sulfide. The size of the boxes and their vertical position are indicative of population densities and depth distribution of the two species as depicted in Fig. 5. Oxygen (○) and sulfide (●) distributions are also depicted.

Below this purple layer with a dominance of chemosynthetic processes, the green and the purple sulfur bacteria coexisted, with a dominance of the latter. With respect to light, interaction between both species is circumented by their almost complementary absorption spectra (Fig. 2). The scalar irradiance measurements indeed confirmed that in the axenic cultures, photons of wavelengths not absorbed by the growing strain were significantly less attenuated with depth and remained potentially available for growth of its counterpart used in the interaction experiment (Fig. 2). Accordingly, the mixed culture showed strong attenuation over the whole spectrum (Fig. 2C).

The coexisting bacteria were located below the maximal oxygen penetration depth; hence, their metabolism was

strictly photolithotrophic. Concerning the possibility of dark metabolism, previous observations suggested that *T. roseopersicina* is able to reduce its intracellular elemental sulfur to sulfide with the catabolism of glycogen to acetate [1 glycosyl unit + 4 S $\rightarrow$ 2 acetate + 2 CO_2 + 4 H_2S], likely representing a rather efficient dark energy generation mechanism (De Wit, Ph.D. thesis, Groningen, The Netherlands). However, a net sulfide production was not detectable from the measured steady state profiles.

During the light period (Fig. 6B), sulfide was oxidized by photolithotrophy to elemental sulfur, which is stored as intracellular globules in Chromatiaceae such as *T. roseopersicina,* whereas in Chlorobiaceae such as *P. aestuarii,* this compound is deposited extracellularly. It is hypothesized that this extracellular elemental sulfur plays a role in the interaction between the bacteria. The extracellular elemental sulfur can react abiotically with sulfide to produce polysulfides [S_x^{2-}] [53]. *T. roseopersicina* is able to use polysulfides with an affinity almost equal to the value found for sulfide [52]. For *Chlorobium* species, polysulfide oxidation is inhibited by sulfide; moreover, this process requires *de novo* protein synthesis [47, 53]. The same type of polysulfide oxidation and its regulation may be tentatively inferred for *P. aestuarii,* because this species is physiologically very similar to *Chlorobium* [4, 12].

The reduction of *P. aestuarii* as compared to the axenic reference culture reflects directly the effects of the partition of sulfide between the two species, when they are cultured together and compete for sulfide. A previous study [37] showed indeed that biomass yield of axenic *P. aestuarii* in the gradient chamber during the incubation period was limited by diffusive delivery of sulfide rather than by radiation energy. In contrast, the important increase of *T. roseopersicina* by comparison with the axenic reference culture is surprising, but can be explained by different hypothesis. In the axenic culture, during the entire light period, the sulfidic zone extended into the layer where the maximum density of *T. roseopersicina* was found. Hence, sulfide was always available for the bacteria, which oxidized it to elemental sulfur stored intracellularly (yielding 2 reducing equivalents per mole of H_2S oxidized). In the mixed culture, the sulfidic zone was located below the biofilm peak at the end of the light period, because of enhanced sulfide consumption by the coculture of both species. Hence, sulfide was depleted during daytime, which favored a complete oxidation of sulfide to sulfate (yielding 8 reducing equivalents per mole of H_2S oxidized) [7, 8]. Thus, a more complete sulfide oxidation resulted in a significant increase of phototrophic yield on sulfide. In addition, the loss of sulfide for the purple sulfur bacteria could be compensated by a flow of S-atoms via polysulfides formed, by the reaction of sulfide and extracellular sulfur of *P. aestuarii,* or via other reduced sulfur compounds, including elemental sulfur, sulfite, and thiosulfate, which are suitable substrates for *T. roseopersicina* strain EP 2204. In contrast, the metabolism of *P. aestuarii* strain CE 2401 is more restricted. Growth is possible with elemental sulfur, but does not occur with thiosulfate and is inhibited by sulfite [12]. In addition, the likely requirement for induction of polysulfide utilization by *P. aestuarii* (see above) favors *T. roseopersicina* in the mixed culture.

To our knowledge, this is the first experimental study on interactions between PSB and GSB, under conditions mimicking their natural habitat, i.e., sand exhibiting pronounced gradients of light and chemical compounds. The combination of this technique and observations in liquid cultures is a powerful tool for understanding growth of and interactions between different species in spatially ordered environments. Our results from the gradient chamber experiments support observations from natural benthic environments, where the purple sulfur bacterium *T. roseopersicina* is often the dominant anoxygenic phototroph [48, 52], and point to a possible importance of coexistence of PSB and GSB in benthic environments and the regulatory mechanisms behind. In view of these results, the study of growth of GSB in benthic environments deserves more attention, as their coexistence with purple sulfur bacteria may be masked by predominance of the latter. Green sulfur bacteria, being obligate anaerobic phototrophs, can only occur in the permanently anoxic part of the sediment if sufficient light is present. These conditions were found in the BGC below 2.2 mm depth and showed that *T. roseopersicina* and *P. aestuarii* can coexist. However, in microbial mats, oxygen production by cyanobacteria may thus limit the proliferation of GSB. An exception is found in the multilayered microbial mats of Great Sippewissett salt marsh, Cape Cod, USA [27, 34, 35]. In these systems, a deep layer (6–7 mm) of the green sulfur bacterium *P. aestuarii* developed underneath two distinct layers of purple sulfur bacteria. The chemolithotrophic activity of the purple bacteria consumed oxygen and presumably prevented the downward diffusion of oxygen into the green layer. Although no data on oxygen microdistribution are available, it seems most likely that the layer of GSB was permanently anoxic. Further investigations are needed to address the role and dynamics of different sulfur compounds, especially elemental sulfur and polysulfides. Measurements of the microdistribution of the different sulfur

species in combination with microsensor measurements would thus further elucidate the microbial interactions governing the coexistence and competition between purple and green sulfur bacteria.

Acknowledgments

Olivier Pringault thanks Professor Bo Barker Jørgensen and Professor Friederich Widdel for the opportunity to stay at the Max Planck Institute für Marine Mikrobiologie (Bremen, Germany) during a period of 4 months. Helle Ploug and Ferran Garcia-Pichel are thanked for discussions of the light measurements. Technicians of the Microsensor Research Group, and particularly Gaby Eickert, are thanked for their effort with microsensor construction. Olivier Pringault was supported by fellowships from the French Ministry of Higher Education and Research (MESR) and the German "Deutscher Akademischer Austausschdienst" (DAAD). Part of this study was supported by the Red-Sea Program project E, "Microbial activities in hypersaline interfaces controlling nutrient fluxes," financed by the German Ministry for Research and Development (BMBF).

References

1. Amesz J (1991) Green photosynthetic bacteria and Heliobacteria. In: Shively JM, Barton LL (eds) Variations in Autotrophic Life, Academic Press, London, pp 99–104
2. Berner RJ (1980) Early Diagenesis: A Theoretical Approach. Princeton University Press, Princeton, NJ
3. Caldwell DC, Wolfaardt GM, Korber DR, and Lawrence JR (1997) Do bacterial communities transcend Darwinism? Adv Microbial Ecol 15:105–191
4. Caumette P (1989) Ecology and general physiology of anoxygenic phototrophic bacteria in benthic environments. In: Cohen Y, Rosenberg E (eds) Microbial Mats, Physiological Ecology of Benthic Microbial Communities, American Society for Microbiology, Washington DC, pp 283–304
5. De Wit CT (1960) On competition. Agricultural Research. Reports (Versl. Landbouwk. Onderz) 66.8, Wageningen, The Netherlands, 88 pp
6. De Wit R, Van Gemerden H (1987) Chemolithotrophic growth of the phototrophic sulfur bacterium *Thiocapsa roseopersicina*. FEMS Microbiol Ecol 45:117–126
7. De Wit R, Van Gemerden H (1990) Growth and metabolism of the purple sulfur bacterium *Thiocapsa roseopersicina* under combined light/dark and oxic/anoxic regimens. Arch Microbiol 154:459–464
8. De Wit R, Van Gemerden H (1990) Growth and metabolism of the purple sulfur bacterium *Thiocapsa roseopersicina* under oxic/anoxic regimens in the light. FEMS Microbiol Ecol 73: 69–76
9. Fischer C, Wiggli M, Schanz F, Hanselmann KW, Bachofen R (1996) Light environment and synthesis of bacteriochlorophyll by populations of *Chromatium okenii* under natural environmental conditions. FEMS Microbiol Ecol 21:1–9
10. Garcia HE, Gordon LI (1992) Oxygen solubility in sea-water: better fitting equations. Limnol Oceanogr 39:462–467
11. Guerrero R, Montesinos E, Pedros-Alio C, Esteve I, Mas J, Van Gemerden H, Hoffman PAG, Bakker JF (1985) Phototrophic sulfur bacteria in two Spanish lakes: vertical distribution and limiting factors. Limnol Oceanogr 30:919–931
12. Guyoneaud R, Matheron R, Baulaigue R, Podeur K, Hirschler A, Caumette P (1996) Anoxygenic phototrophic bacteria in eutrophic coastal lagoons of the French Mediterranean and Atlantic Coasts (Prévost Lagoon, Arcachon Bay, Certes Fishponds). Hydrobiol 329:33–43
13. Herbert RA, Welsh DT (1994) Establishment of phototrophic purple sulfur bacteria in microbial mat systems. In: Stal LJ, Caumette P (eds) Microbial Mats: Structure, Development and Environmental Significance. NATO ASI Ser. Vol. G35, Springer-Verlag, Berlin, pp 51–60
14. Imhoff JF (1995) Taxonomy and physiology of phototrophic purple bacteria and green sulfur bacteria. In: Blankenship RE, Madigan MT, Bauer CE (eds) Anoxygenic Photosynthetic Bacteria. Kluwer Academic Publishers, The Netherlands, pp 1–15
15. Jeroschewski P, Steuckart C, Kühl M (1996) An amperometric microsensor for the determination of H_2S in aquatic environments. Anal Chem 68:4351–4357
16. Kämpf C, Pfennig N (1986) Chemoautotrophic growth of *Thiocystis violacea* and *Chromatium gracile* and *C. vinosum* in the dark at various O_2 concentrations. J Basic Microbiol 26: 517–531
17. Kirk JTO (1994) Light and Photosynthesis in Aquatic Ecosystems, 2nd ed. Cambridge University Press, Cambridge
18. Kohler HP, Ahring B, Abella C, Ingvorsen K, Keweloh H, Laczko E, Stupperhich E, Tomei F (1984) Bacteriological studies on the sulfur cycle in the anaerobic part of the hypolimnion and in the surface sediments of Rotsee in Switzerland. FEMS Microbiol Lett 21:279–289
19. Kühl M, Jørgensen BB (1992) Spectral light measurements in microbenthic phototrophic communities with a fiber-optic microprobe coupled to a sensitive diode array detector. Limnol Oceanogr 37:1813–1823
20. Kühl M, Jørgensen BB (1992) Microsensor measurements of sulfate reduction and sulfide oxidation in compact microbial communities of aerobic biofilms. Appl Environ Microbiol 58: 1164–1174
21. Kühl M, Jørgensen BB (1994) The light field of microbenthic communities: radiance distribution and microscale optics of sandy coastal sediments. Limnol Oceanogr 39:1368–1398
22. Kühl M, Lassen C, Jørgensen BB (1994) Light penetration and light intensity in sandy marine sediments measured with ir-

radiance and scalar irradiance fiber-optic microprobes. Mar Ecol Prog Ser 105:139–148
23. Kühl M, Lassen C, Jørgensen BB (1994) Optical properties of microbial mats: light measurements with fiber-optic microprobes. In: Stal LJ, Caumette P (eds) Microbial mats: structure, development and environmental significance. NATO ASI Ser. Vol. G35, Springer-Verlag, Berlin, pp 149–157
24. Kühl M, Steuckart C, Eickert G, Jeroschewski P (1998) A H_2S microsensor for profiling biofilms and sediments: Application in an acidic lake sediment. Aquat Microbial Ecol 15:201–209
25. Lassen C, Ploug H, Jørgensen BB (1992) A fibre-optic scalar irradiance microsensor: application for spectral light measurements in sediments. FEMS Microbiol Ecol 86:247–254
26. Madigan MT (1988) Microbiology, physiology, and ecology of phototrophic bacteria. In: Zehnder A (ed) Biology of Anaerobic Microorganisms. John Wiley & Sons, New York, pp 11–39
27. Nicholson JA, Stolz JF, Pierson BK (1987) Structure of microbial mat at Great Sippewisset Marsh, Cape Cod, Massachussets. FEMS Microbiol Ecol 45:343–364
28. Nielsen LP, Christensen PB, Revsbech NP, Sørensen J (1990) Denitrification and oxygen respiration in biofilms studied with a microsensor for nitrous oxide and oxygen. Microb Ecol 19:63–72
29. Oren A, Kühl M, Karsten U (1995) An endoevaporitic microbial mat within a gypsum crust: zonation of phototrophs, photopigments, and light penetration. Mar Ecol Prog Ser 128: 151–159
30. Overmann J, Cypionka H, Pfennig N (1992) An extremely low-light-adapted phototrophic sulfur bacterium from the Black Sea. Limnol Oceanogr 37:150–155
31. Overmann J, Pfennig N (1992) Continuous chemotrophic growth and respiration of Chromatiaceae species at low oxygen concentrations. Arch Microbiol 158:59–67
32. Parkin TB, Brock TD (1980) The effects of light quality on the growth of phototrophic bacteria in lakes. Arch Microbiol 125: 19–27
33. Pfennig N, Trüper HG (1992) The family Chromatiaceaea. In: Balows A, Trüper HG, Dworkin M, Harder W, Schleifer KH (eds) The Prokaryotes, 2nd ed., Springer-Verlag, New York, pp 3200–3221
34. Pierson BK, Oesterle A, Murphy GL (1987) Pigments, light penetration and photosynthetic activity in the multi-layered microbial mats of Great Sippewissett salt marsh. FEMS Microbiol Ecol 45:365–376
35. Pierson BK, Sands VM, Frederick JL (1990) Spectral irradiance and distribution of pigments in a highly layered marine microbial mat. Appl Environ Microbiol 56:2327–2340
36. Pringault O, De Wit R, Caumette P (1996) A Benthic Gradient Chamber for culturing phototrophic sulfur bacteria on reconstituted sediments. FEMS Microbiol Ecol 20:237–250
37. Pringault O, Kühl M, De Wit R, Caumette P (1998) Growth of green sulfur bacteria in experimental benthic oxygen, sulphide, pH and light gradients. Microbiology 144:1051–1061
38. Rasmussen H, Jørgensen BB (1992) Microelectrode studies of seasonal oxygen uptake in a coastal sediment: role of molecular diffusion. Mar Ecol Prog Ser 81:289–303
39. Revsbech NP (1989) An oxygen microsensor with a guard cathode. Limnol Oceanogr 34:472–476
40. Revsbech NP, Jørgensen BB (1986) Micro-electrodes: their use in microbial ecology. Adv Microb Ecol 9:293–352
41. Schmidt K (1978) Biosynthesis of carotenoids. In: Clayton RK, Sistrom WR (eds) The Photosynthetic Bacteria. Plenum Publishing Corp, New York, pp 729–750
42. Sirevåg R (1995) Carbon metabolism in green bacteria. In: Blankenship RE, Madigan MT, Bauer CE (eds) Anoxygenic Photosynthetic Bacteria. Kluwer Academic Publishers, The Netherlands, pp 871–883
43. Stal LJ, Van Gemerden H, Krumbein WE (1985) Structure and development of benthic marine microbial mat. FEMS Microbiol Ecol 31:111–125
44. Tabita FR (1995) The biochemistry and metabolic regulation of carbon metabolism and CO_2 fixation in purple bacteria. In: Blankenship RE, Madigan MT, Bauer CE (eds) Anoxygenic Photosynthetic Bacteria. Kluwer Academic Publishers, The Netherlands, pp 885–914
45. Van Gemerden H (1984) The sulfide affinity of phototrophic bacteria in relation to the location of elemental sulfur. Arch Microbiol 139:289–294
46. Van Gemerden H (1986) Production of elemental sulfur by green and purple sulfur bacteria. Arch Microbiol 146:52–56
47. Van Gemerden H (1987) Competition between purple sulfur bacteria and green sulfur bacteria: role of sulfide, sulfur and polysulfides. Acta Academiae Aboensis 47:13–27
48. Van Gemerden H (1993) Microbial mats: a joint venture. Mar Geol 113:3–25
49. Van Gemerden H, Mas J (1995) Ecology of phototrophic sulfur bacteria. In: Blankenship RE, Madigan MT, Bauer CE (eds) Anoxygenic Photosynthetic Bacteria. Kluwer Academic Publishers, The Netherlands, pp 49–85
50. Van Gemerden H, Tughan CS, De Wit R, Herbert RA (1989) Laminated microbial ecosystems of sheltered beaches in Scapa flow, Orkney Islands. FEMS Microbiol Ecol 62:87–102
51. Veldhuis MJW, Van Gemerden H (1986) Competition between purple and brown phototrophic bacteria in stratified lakes: sulfide, acetate, and light as limiting factors. FEMS Microbiol Ecol 38:31–38
52. Visscher PT, Nijburg JW, Van Gemerden H (1990) Polysulfide utilization by *Thiocapsa roseopersicina.* Arch Microbiol 155: 75–81
53. Visscher PT, Van Gemerden H (1988) Growth of *Chlorobium limicola* f. *thiosulfatophilum* on polysulfides. In: Olson JM, Jormerod JG, Amesz J, Stackebrandt J, Trüper HG (eds) Green Photosynthetic Bacteria. Plenum Press, New York, pp 287–294